Desalination and Water Treatment
www.deswater.com
doi: 10.1080/19443994.2015.1125796

57 (2016) 21377–21390
September

Taylor & Francis
Taylor & Francis Group

Analysis of variables affecting mixed liquor volatile suspended solids and prediction of effluent quality parameters in a real wastewater treatment plant

Majid Bagheri[a,*], Sayed Ahmad Mirbagheri[a], Majid Ehteshami[a], Zahra Bagheri[b], Ali Morad Kamarkhani[c]

[a]*Department of Civil Engineering, K.N. Toosi University of Technology, Tehran, Iran, Tel. +98 9181331137; Fax: +98 2188770006; email: bagherimajead@yahoo.com (M. Bagheri), Tel. +98 9121374357; email: Mirbagheri@kntu.ac.ir (S.A. Mirbagheri), Tel. +98 9121147833; email: Eht_mj@yahoo.com (M. Ehteshami)*
[b]*Department and Faculty of Basic Sciences, PUK University, Kermanshah, Iran, Tel. +98 8325245574; email: zahra90_bagheri@yahoo.com*
[c]*Department of Chemical Engineering, Razi University, Kermanshah, Iran, Tel. +98 9186171061; email: Ali.ka1361@gmail.com*

Received 12 April 2015; Accepted 25 October 2015

ABSTRACT

This article was an effort to predict effluent quality parameters and analyze variables affecting mixed liquor volatile suspended solids (MLVSS) for Ekbatan wastewater treatment plant in Tehran, Iran. These parameters were predicted and analyzed using two of the most common classes of artificial neural networks (MLP and RBF) coupled with genetic algorithm. Temperature, pH, influent concentration of the parameters, sludge volume index (SVI), and sludge volume after 30 min of settling (V30) were inputs of the neural networks. These inputs were used to predict biochemical oxygen demand (COD), total nitrogen (TN), and total suspended solids (TSS) concentrations as well as MLVSS concentration in the aeration tank. The introduced models for training and testing data sets indicated an almost perfect match between the experimental and the predicted values of COD, TN, TSS, and MLVSS. The models were verified by evaluating their performance in propitiously simulating the statistical features of the observed data. Furthermore, another criterion applied for judging the validity of the models was the assessment of the goodness of fit according to available criteria. The mean average error in prediction of all parameters for the train and test models did not exceed 6 and 4%, respectively. The results of sensitivity analyses for the models indicated that the variation of the MLVSS concentration in the aeration tank is influenced by V30, influent TSS, T (°C), SVI and pH, respectively. It was observed that the V30 and influent TSS significantly affect the MLVSS concentration in the aeration tank.

Keywords: Artificial neural network; Genetic algorithm; Multi-layer perceptron; Radial basis function; Wastewater treatment plant

1. Introduction

Activated sludge plant is usually difficult to operate and control because of its complex operational behavior and usual significant process disturbances [1]. Stringent discharge standards and time-dependent non-uniform influent characteristics make the proper management of treatment systems an issue [2,3]. To increase safety and to improve operating performance

*Corresponding author.

of this biological wastewater treatment process, it is important to develop computer operational decision support systems. These intelligent computing systems are able to assist ordinary operators to work at the level of a domain expert in daily operation [1]. There are several models for the biological wastewater treatment in the literature based on the fundamental biokinetics such as activated sludge model No. 1 (ASM1) [3]. These types of models integrate many of the key biological, physical, and chemical processes within the activated sludge process (ASP) into a form that can predict the behavior of wastewater treatment plants (WWTP) [4]. The ASM2 models extended the capabilities of ASM1 to involve the biological phosphorus and nitrogen removals [5], whereas, ASM3 introduced an alternative concept to the previous ASM biokinetics and aimed at simplifying the model application [6]. The diagnosis of the process interactions and modeling of ASP are still difficult due to the complex biological reactions, as well as the highly time-varying and multivariable aspects of operation in a real WWTP [7]. Furthermore, more advanced control methods need models for the controller design and tuning and face the problems with parameter identification of nonlinear activated sludge models [4].

The artificial neural networks (ANNs) have been used for monitoring, controlling, classification, and simulation [8,9] of ASPs of WWTPs [10–14]. A summary of the applications of ANN modeling in a real WWTP is given in Table 1. So far, different types of neural networks have been used, and their performances have been studied for the purpose of modeling in different engineering issues. The frequently used networks include multi-layer perceptrons (MLPs), radial basis functions (RBFs), recurrent neural networks (RNNs), and echo-state networks (ESNs). The MLP and RBF are two types of feed-forward artificial neural networks (FANNs), which are most commonly used in classification problems [15]. Moral et al. [2] developed MLP artificial neural networks (MLPANNs) to model ASP for two different cases. The input and output data for the training of the ANN models were generated using a simulation model, which was an implementation of the ASM1. The results showed high correlation coefficient between the observed and predicted output variables. Mjalli et al. [16] introduced an MLPANN modeling approach to acquire the knowledge base of a real wastewater plant, and then used it as a process model. They showed that the MLPANNs are capable of capturing the plant operation characteristics with a good degree of accuracy. The model provided accurate predictions of the effluent stream, in terms of biological oxygen demand (BOD), chemical oxygen demand (COD), and total suspended solids (TSS) when using COD as an input in the crude supply stream. Han et al. [17] applied RBF artificial neural networks (RBFANNs) in order to model and control dissolved oxygen (DO) concentration in activated sludge wastewater treatment processes. The results indicated that RBFANN effectively provides process control. The performance comparison also showed that the proposed model's predictive control strategy yields the most accurate for DO concentration. The main advantage of ANN models [18–21] is due to nonlinear mapping of ANN from input to output sets as well as complexity of interaction between neurons. Zilouchian and Jafar [12] mentioned that the utilization of an RBFANN model to predict the product quality of reverse osmosis process is a key factor to decrease the membrane degradation and to increase the overall efficiency of the system.

Utilizing an appropriate optimization approach in combination with the ANN models is useful and leads to the determination of optimal input parameters in maximization or minimization purposes [22]. Genetic algorithm (GA) is a search heuristic that mimics the process of natural evolution and applies the natural selection processes, where selection results in better fitted species [23]. This method can find optimal solutions in a large solution space by evaluating only a relatively small number of potential solutions. It works directly with the fitness of each solution instead of derivatives or other auxiliary characteristics used with traditional deterministic approaches [24]. The number of solutions is one of the important parameters that influence optimization by GA. By increasing the population size, more solutions will be investigated, covering a wider area of the solution space, thus increasing the probability of finding the optimal solution in each generation [25]. GA can be used to optimize the weights and thresholds of ANN for minimizing the error between the actual and target outputs [26]. The GA-based ANN models have not been reported in the prediction of effluent quality parameters and analysis of mixed liquor volatile suspended solids (MLVSS) in a real WWTP.

This study describes the development of two GA-based ANN models to accurately predict effluent COD, TSS and total nitrogen (TN), and MLVSS for Ekbatan WWTP under various operating parameters. The operating parameters include pH, temperature (T), influent TSS, sludge volume index (SVI), and sludge volume after 30 min of settling (V30). The influent COD or TN was used instead of influent TSS in order to predict effluent COD or TN in the modeling process. Due to the dependence of SVI upon sludge concentration, the V30 was measured in the

Table 1
Summary of researchers studies in ANN modeling of a WWTP

The purpose of applying ANN	ANN	Researcher (s)
Modeling of activated sludge process in a WWTP	MLP	Moral et al. [2]
Prediction of WWTPs performance in terms of COD, BOD, and TSS	MLP	Mjalli et al. [16]
Prediction of activated sludge bulking in a WWTP	RBF	Han and Qiao [10]
Forecasting effluent quality of an industry WWTP	MLP	Chen et al. [11]
Automation and process control of reverse osmosis plants	RBF	Zilouchian and Jafar [12]
A predictive control system for the coagulation process in a paper mill WWTP	MLP	Zeng et al. [13]
To predict the performance of WWTP in terms of COD, BOD, and TSS	MLP	Nasr et al. [14]
To model a municipal WWTP in terms of BOD and TSS	MLP	Hamoda et al. [18]
Prediction of suspended solids and COD in hospital WWTP effluent	MLP	Pai et al. [9]
Formal verification of WWTPs using events detected from continuous signals	MLP	Luccarini et al. [19]
To model predictive control of DO concentration in activated sludge WWTPs	RBF	Han et al. [17]
Prediction of WWTP performance in term of TSS	MLP	Hanbay et al. [20]
Real-time remote monitoring of small-scaled biological WWTPs	MLP	Lee et al. [7]
To predict the elimination of total organic carbon (TOC) in an industrial WWTP	MLP	Gontarski et al. [21]
For rapid WWTP performance evaluation: Methodology and case study	MLP	Raduly et al. [8]

Ekbatan WWTP for an objective comparison of the effect of additives on sludge settling. The variables affecting the MLVSS concentration in the aeration tanks were also analyzed in order to determine their importance order and their effect in the results of introduced models.

2. Materials and methods

2.1. Features and operating conditions of Ekbatan WWTP

Ekbatan WWTP is located in Tehran, Iran. The WWTP covers a population of about 100,000 people. The WWTP treats wastewater with an average capacity of about 4,500 m^3/d. The influent wastewater is treated in the WWTP using anaerobic-anoxic-oxic (A2O) method. Fig. 1 shows that the Ekbatan WWTP comprises fine and coarse screens, grid removal, pretreatment unit, anaerobic tanks, anoxic tanks, activated sludge aeration tanks, secondary sedimentation tanks, and disinfection unit. The influent wastewater initially passes through the fine and coarse screens and then enters to the grit removal phase. When wastewater enters to the grit chamber, the particles slow down and crash due to their collision with chamber wall. The inorganic matters settle in the grit chamber with a hydraulic retention time (HRT) of 2–3 min, and the HRT sometimes changes from 15 to 20 min to function like a primary clarifier. After pretreatment processes, the wastewater enters to anaerobic tanks with a HRT of 0.5 h and then enters to anoxic tank. The anoxic phase is finished with a HRT of 2 h, and then wastewater enters to the aeration tank. The subsurface aeration is performed in the aeration tank with a HRT of 8 h, and then the wastewater enters to secondary clarifier. The effluent is disinfected at the end of process.

2.2. Wastewater analysis

Analysis of the wastewater characteristics in Ekbatan WWTP is carried out daily, weekly, and monthly. BOD, COD, nitrate (NO_3^+-N), ammonia (NH_4^+-N), TN, TSS, total dissolved solids (TDS), mixed

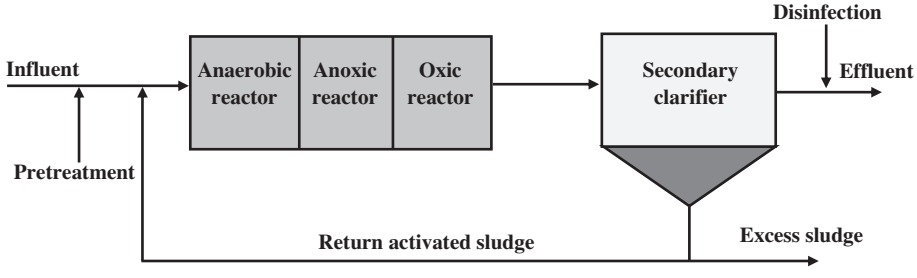

Fig. 1. Configuration of the process used in the Ekbatan WWTP.

liquor suspended solids (MLSS), MLVSS, SVI, V30 as well as pH, T (℃), and DO are measured in Ekbatan WWTP. The pH and T (℃) are measured using a digital pH meter. A dissolved oxygen meter (YSI 5000) is utilized to determine DO. COD and biodegradability, which is determined by 5-d biochemical oxygen demand (BOD_5) test, are measured according to the standard methods [27]. Weekly analyses are included MLVSS and MLSS in aeration reactors. MLSS and MLVSS are determined in Ekbatan WWTP laboratory at the temperature of 550℃ [28]. In the WWTP laboratory, TN, NH_4^+-N, and NO_3^+-N are measured using a spectrophotometer (the Hach DR 5000 UV–vis Laboratory Spectrophotometer). Based on the results of wastewater analysis, it was observed that the wastewater characteristics, including influent COD, TN, T (℃), and TSS as well as other parameters, including MLVSS, V30, and SVI have significantly varied from 2011 to 2013. Table 2 shows the influent raw wastewater characteristics and other parameters related with the operation of Ekbatan WWTP.

2.3. Artificial neural network modeling approach

ANN is a nonparametric model which utilizes interconnected mathematical nodes or neurons to form a network that can model complex functional relationships [8]. Such models permit to study the relationship between the input variables and the target(s) or output(s) of the process using a limited number of experimental runs. ANNs have been proved to be able to model nonlinear systems and successfully applied for modeling various nonlinear processes [19].

Table 2
Daily influent wastewater characteristics and other parameters of Ekbatan WWTP

Parameter (unit)	Average	Standard deviation
T_{inf} (℃)	23	2.8
pH_{inf} (℃)	8.2	0.4
BOD_{inf} (mg/L)	153	27
COD_{inf} (mg/L)	211	35
TN_{inf} (mg/L)	29	4
NH_4^+-N_{inf} (mg/L)	18	3
NO_3^+-N_{inf} (mg/L)	0.8	0.2
TDS_{inf} (mg/L)	460	61
TSS_{inf} (mg/L)	191	32
V30 (ml/L)	301	112
SVI (ml/g)	171	49
MLVSS (mg/L)	1,562	281
TSS_{out} (mg/L)	10	4
COD_{out} (mg/L)	15	3
TN_{out} (mg/L)	2	0.2

The ANNs operating in parallel being composed of neurons. An artificial neuron is a single computational processor, which has two operators (1) summing junction and (2) transfer function [15,29]. The connections consist of weights and biases with neurons addressing information. Considering the model of a single neuron, any scalar input x_i is transmitted via a connection that multiplies its strength by the scalar weight w_i to form the product $w_i \times x_i$. The bias b is much like a weight, except that it has a constant input of unity and it is simply added to the product $w_i \times x_i$ by summing junction [29]. The transfer function determines the input/output behavior and adds nonlinearity and stability to the network [13]. It takes the argument z and produces the scalar output of a single neuron [18]. The linear function (purelin) and hyperbolic tangent sigmoid function (tansig) are the most used transfer functions to solve linear and nonlinear problems, and can be described by Eqs. (1) and (2), respectively.

$$\text{purlin}(z) = z \tag{1}$$

$$\text{tansig}(z) = 2/(1 + e^{-2z}) - 1 \tag{2}$$

2.4. Architecture of RBFANN and MLPANN

Recently, the use of ANNs is also gaining popularity in modeling biological wastewater treatment processes [14,17]. MLP and RBF are two types of feed-forward ANNs, which are most commonly used in the simulation of biological wastewater treatment processes, namely prediction of a WWTP performance. In these feed-forward networks, the data are only transmitted in the forward direction from the input layer to the hidden layer and to the output layer. The structure of the basic RBFANN used in this study consists of one input layer, one output layer, and one hidden layer (Fig. 2(b)). The RBFANNs have a very strong mathematical foundation rooted in regularization theory for solving ill-conditioned problems. An RBFANN has a simple neural network structure in terms of the direction of information flow, and the performance of an RBFANN is heavily dependent on its architecture [4]. A single-output RBFANN with N hidden layer nodes can be described by Eqs. (3) and (4):

$$Y = \sum_{n=1}^{N} w_n \theta_n(X) \tag{3}$$

where X and Y are the input and output of the network, $X = (x_1, x_2, \ldots, x_m)^T$, w_n is the connecting weights between nth hidden node and the output layer, θ_n is the output value of the nth hidden node, and

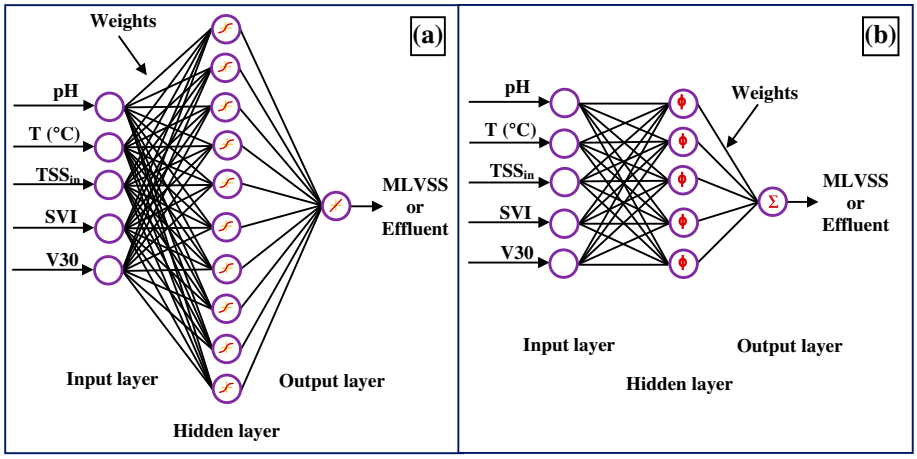

Fig. 2. Topological architectures of the neural networks used in this study: MLP (a) and RBF (b).

$$\theta_n(X) = e^{(-||x-\mu_n||/\sigma_n^2)} \tag{4}$$

where μ_n is the center vector of nth hidden node, $||x-\mu_n||$ is the Euclidean distance between x and μ_n, and σ_n is the radius of the nth hidden node.

The MLPANN is formed by simple neurons called perceptron. The structure of the basic MLPANN consisted of one input layer, one output layer, and one hidden layer (Fig. 2(a)). The input neurons receive the data values and pass them on to the first hidden layer neurons. Each one collects the input from all input neurons after multiplying each input value by a weight, attaches a bias to this sum, and passes on the results through a nonlinear transfer function. This forms the input either for the second hidden layer or the output layer that operates identically to the hidden layer. The resulting transformed output from each output neuron is the network output [30]. A single-output MLPANN with N hidden layer nodes can be described by Eq. (5):

$$Y = f\left(\sum_{n=1}^{N} w_n X_n + b\right) \tag{5}$$

where w_n is the weight vector, X_n is the input vector ($n = 1, 2, \ldots, N$), b is the bias, f is the transfer function, and Y is the output.

The performances of the ANN models were measured by coefficient of determination (R^2) and root-mean-squared error (RMSE) between the predicted values of the network and the experimental values, which were calculated by Eqs. (6) and (7), respectively [31]:

$$R^2 = 1 - \sum_{i=1}^{n}(y_i^* - y_p^{(i)})^2 / \sum_{i=1}^{n}(y_i^* - \bar{y})^2 \tag{6}$$

$$\mathrm{RMSE} = \sqrt{\frac{1}{n}\sum_{i=1}^{n}(y_p^{(i)} - y_i^*)^2} \tag{7}$$

where $\bar{y}$ is the average of y over the n data, and y_i^* and $y_p^{(i)}$ are the ith target and predicted responses, respectively.

2.5. Genetic algorithm optimization approach

GA is a search heuristic and is a type of evolutionary algorithm. Many applications have been developed using genetic algorithms [22]. Basically, a GA is categorized into four main steps: (1) creating population: the numbers of the initial populations are generated in this step, (2) selection: the solution for creating the offspring is chosen in this step, (3) crossover: this section is dedicated to creating new solutions by considering the solutions from the selection step, (4) mutation: a sudden change in a step of the solution's feature is called mutation [23]. The GA is started with a set of random solutions called population [4]. Solutions from one population are used to form a new population [32]. This is motivated by a hope that the new population will be better than old population. In order to form a new population, GAs use genetic operators and selection process [4]. Genetic operators are used to generate the new solutions (offspring) from the current solutions (parents).

Selection is the process of keeping and deleting some solutions from both parents and off-spring for the same number of next population [33]. There are different selection methods as stochastic uniform, remainder, uniform, shift linear, roulette wheel and tournament [34]. The tournament method is preferred and can be described by Eq. (8):

$$\tau_i = F_i / \sum_{j=1}^{N_k} F_j \tag{8}$$

where τ_i is the weight of ith individual within population. Moreover, the sum of the elective probabilities of all the individuals within population is 1 as is determined by Eq. (9):

$$\sum_{i=1}^{N_k} \tau_i = 1 \tag{9}$$

Crossover is a key genetic operator for GA convergence. It is applied on two individuals, called parents, and originates two new individuals called sons, which contain the combined traits of the parents [4]. Parents are taken from the mating pool, which is filled with individuals of the original population, using the selection process. The number of parents selected for crossover is dictated by the crossover rate [35]. The value of 1 and 0 as gen number of an individual is randomly produced. If the value is 1, then gen is taken from mother, and if the value is 0, then gen is taken from father and thus the child is produced [34].

In mutation stage, new individuals are produced to be changed all or some gens of the selected individuals within population [36,37]. Even though genetic algorithms have less chance of getting trapped in local minima, sometimes a premature convergence can occur. To prevent it, genetic variability has to be maintained. The mutation operator is one of the strategies used to ensure variability within the population and design space exploration [38]. Mutation is applied in the offspring generated by the crossover with a mutation probability p_m to which low values are usually assigned. For each layer of the chromosome, a random number between 0 and 1 (r) is generated. If such number is lower than the mutation probability, a feasible random integer replaces the original gene value [35].

In this study, the roulette wheel and tournament selection methods, a transformation-based mutation, and single point, double point and uniform crossover methods were used as genetic operators. The selection, mutation, and crossover probabilities were 0.5, 0.15, and 0.35, respectively. In addition, the number of variables, population size, and generation gap were 6, 20, and 1, respectively.

2.6. Data scaling in the modeling process

In order to obtain convergence within a reasonable number of cycles, the input and output data should be normalized and scaled to the range of 0–1 by Eq. (10) [39]:

$$x_{\mathrm{ni}} = (x_i - x_{\min})/(x_{\max} - x_{\min}) \tag{10}$$

where x_i is the initial value, $x_{\max}$ and $x_{\min}$ are the maximum and minimum of the initial values, and x_{ni} is the scaled value. After the training and testing of the ANN, the output data were scaled to the real-world values through Eq. (11):

$$x_i = x_{\mathrm{ni}}(x_{\max} - x_{\min}) + x_{\min} \tag{11}$$

Simulation models of operational parameters were established based on the theory of FANN using the mathematical software program, MATLAB. Experimental data obtained over three years (2011–2013) were used in ANN modeling. The statistical characteristics of the measured variables are presented in Table 3. The hybrid MLPANN-GA and RBFANN-GA models were developed to accurately predict effluent COD, TSS, and TN, and simulate MLVSS for Ekbatan WWTP.

3. Results and discussion

3.1. Parameter adjustment and preliminary findings

In order to simulate the MLVSS concentration in the aeration tank by RBFANN-GA and MLPANN-GA, pH, T (˚C), influent TSS, SVI, and V30 were considered as inputs of the networks. Each ANN structure was selected after running a number of preliminary experiments to explore the training speed and response time of different architectures. To keep the ANN structure as simple as possible, three layers were used in all networks. The RBFANN applied different network functions such as newrbe and newrb to the input data. The newrb function designs a radial basis neural network, and the newrbe function designs an exact radial basis ANN. The MLPANN applied different network functions such as newff to the input data. The newff function designs a feed-forward back-propagation neural network. The MLPANN was trained by different learning algorithms (including incremental back propagation, gradient descent

Table 3
Characteristics of measured variables used for modeling by MLPANN-GA and RBFANN-GA

Input variable no.	Input variable	Range	Avg.	Std.	Output variable	Range	Avg.	Std.
1	pH	6.7–8.9	8.2	0.4	MLVSS (mg/L)	120–3,280	1,562	281
2	*T* (°C)	16.9–28.5	23	2.8	*Effluent*			
3	*Influent*				TSS (mg/L)	1.5–34	10	4
	TSS (mg/L)	22.5–595	191	32	COD (mg/L)	2–42	15	3
	COD (mg/L)	72–400	211	35	TN (mg/L)	0.4–16.2	2	0.2
	TN (mg/L)	15.5–57	29	4				
4	SVI (ml/g)	44–754	171	49				
5	V30 (ml/L)	30–950	301	112				

Notes: Avg.: the average of data sets and Std.: the standard deviation of data sets.

back-propagation (GDB), Levenberg–Marquardt (LM) algorithm, and batch back-propagation). The transfer function of the hidden and output layers is iteratively determined by developing several networks. The optimal architectures insure training with reasonable speed and short simulation time for a specific network performance. The RBFANN regularization network employs the same number of neurons as the input data points. The number of neurons of MLPANNs was kept equal to the number of training exemplars for better comparison of both ANN performances [30]. A two-stage training process was applied for the RBFANNs. The K-means to assign the radial centers in the data set and K-nearest neighbors to compute the deviation of each center were used in the first stage. The output layer was optimized with pseudo-inverse method in the second stage. To determine the best network function, various algorithms were studied. The RBFANN-GA applied network function of newrbe to the input data as optimal function, and the spread of radial basis function was considered equal to its default value, 1 [17]. A large spread value results in a smooth function approximation, but by contrast, a small spread value can results in numerical problems. The network function of newrbe chose 65% of normalized data to train and 35% to test the RBFANN-GA models. The RBFANN-GA was designed in a loop that applied network function of newrbe to the data for less than 100 times in order to minimize error. Optimal network was chosen on the basis of the minimum average error.

The MLPANN-GA applied network function of newff to the input data as optimal function; therefore, it created a feed-forward back-propagation neural network (FBNN). The network function of newff chose 60% of normalized data to train, 20% to test, and 20% to validate the MLPANN-GA models. The MLPANN-GA was trained by different learning algorithms for maximum 400 epochs. Nevertheless, the LM algorithm resulted in the optimal models for training and testing data after less than 20 iterations. In the ANN models, the predictive accuracy of networks depends on the number of hidden neurons, learning functions, and learning rate [29]; so these variables were chosen to optimize the ANN structure by GA program. Based on our research, the optimal models were obtained with the hidden layer consisting of 10 neurons compared with previous researches, which varied from 10 to 80 neurons [2,16,22]. The best transfer function for the hidden layer was found to be hyperbolic tangent sigmoid (tansig) function while the best transfer function for the output layer was a linear one (purelin). The results of two training algorithms, including LM and GDB, and two transfer functions, including hyperbolic tangent sigmoid (tansig) function and pure linear function, were compared in order to determine the effect of GA on the MLPANN-GA models. The RMSE of hyperbolic tangent sigmoid (tansig) transfer function and ten neurons with LM learning algorithm was the lowest value. Moreover, coefficient of determination value of this structure was low. Because gradient descent usually slows down near minima, so the LM method can be used to obtain faster convergence. LM is a blend of simple gradient descent and the Gauss–Newton method [31]. LM has found to be the fastest method for training moderate-sized feed-forward neural networks, where the training rate is 10–100 times faster than the usual GDB method [36]. The hyperbolic tangent sigmoid (tansig) function was selected for hidden neurons due to its better prediction performance than other transfer functions among different transfer functions available in MATLAB.

3.2. Prediction and analysis of MLVSS

Fig. 3 shows that the results of the MLVSS modeling using the RBFANN-GA and MLPANNGA for training and testing data were highly collaborated

with previous studies [2,31]. The training procedures for the simulation of MLVSS concentration in the aeration tank were successful for both RBFANN-GA and MLPANN-GA models. The train and test models by RBFANN-GA and MLPANN-GA showed an almost perfect match between the experimental and the simulated values of MLVSS. It is obvious that an accurate verification is required for the proper use of these models in practical applications [19]. In this research, the models are verified by evaluating their performance in propitiously simulating the statistical features of the measured data. The autocorrelation functions of the simulated values are compared to the measured values. Moreover, another criterion applied for judging the validity of the models is the assessment of the goodness of fit according to different available criteria. The values of R^2 for train and test (verification) models by RBFANN-GA were 0.96126 and 0.93068, respectively. The values of R^2 for train and test models by MLPANN-GA were 0.98285 and 0.95232, respectively. The results indicate a good fitting between simulated values of MLVSS by RBFANN-GA and MLPANN-GA and experimental values for various inputs. It has been demonstrated that the model fit statistics are not a good guide to how well a model will simulate and predict a time-series phenomenon [19]. High values of R^2 do not necessarily result in a favorable model, although it can be a sign of a successful model. Additionally, a way to measure the predictive capability of a model is to test it on a set of data not used in simulation process [3]. This has been described in literature as test set and the data used for simulation is training set [21]. As a result, to verify our models, a set of the MLVSS data was used to investigate the predictive ability of the models. The values of RMSE for train and test models by RBFANN-GA were 92 and 120 mg/L, respectively. The values of RMSE for train and test (verification) models by MLPANN-GA were 85 and 104 mg/L, respectively. The mean average error in simulation of MLVSS by RBFANN-GA and MLPANN-GA for train and test models did not exceed 2 and 1%, respectively.

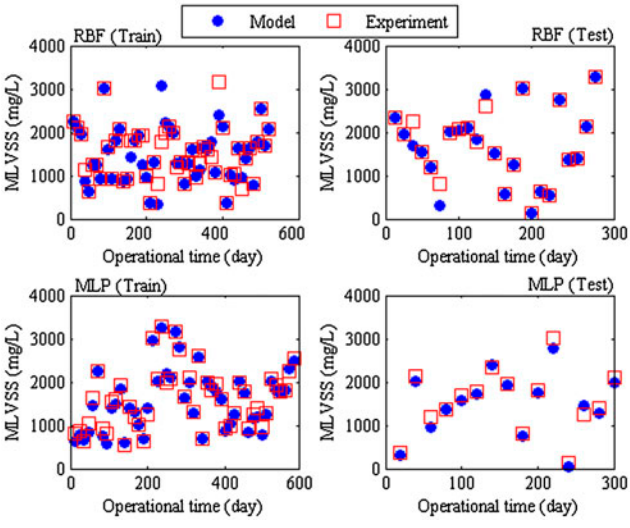

Fig. 3. MLVSS models by RBFANN-GA and MLPANN-GA based on train and test data sets.

Although it is not a common procedure to use an effluent parameter as an input in modeling, in previous studies, various combinations of variables were used to build the ANN models [2]. The input variables were solids retention time, influent flow rate, influent pH, influent water temperature, influent COD, MLSS, effluent TSS, and sludge production rate from the primary sedimentation tank. These variables, alone or in different combinations, were used as the ANN model inputs to predict effluent COD. It was observed that the implementation of the modeling started with the determination of the variable combinations exhibiting better results in ANN model output [16]. For this purpose, in the current research, the MLVSS was modeled separately by considering various single variables as inputs of RBFANN-GA and MLPANN-GA in order to examine the effect of each variable on the changes of MLVSS concentration in the aeration tank. In a similar way, separate models were performed in order to show the effect of joint input variables on the changes of MLVSS concentration in the aeration tank. These inputs were used to train the ANNs in groups of two, three, and four variables. The results showed that V30 among single input variables, and V30 and influent TSS among groups of two variables significantly affected the MLVSS models. Furthermore, V30, influent TSS and T (°C) among groups of three variables, and V30, influent TSS, T (°C), and SVI between groups of four variables had the most significant effects on the MLVSS models (Table 4). Moreover, sensitivity analyses [40] were performed to examine the sensitivity of MLVSS concentration in the aeration tank to changes of input variables. The effect of each variable on the RBFANN-GA and MLPANN-GA models comparing to the other variables was determined by its importance order (its rank). Table 4 shows the importance order of each input variable and the joint variables for the simulation of MLVSS concentration in the aeration tank. The variable with higher rank of importance indicated not only an almost perfect match between experimental and simulated values by both RBFANN-GA and MLPANN-GA models but also less RMSE and more R^2 values. The results of sensitivity analyses for

RBFANN-GA and MLPANN-GA models showed that the variation of the MLVSS concentration in the aeration tank is influenced by V30, influent TSS, T (°C), SVI, and pH. This research indicates that the V30 and influent TSS significantly affect the MLVSS concentration in the aeration tank.

Both RBFANN-GA and MLPANN-GA showed similar results for the models with single input variables and joint variables. It was observed that the precision of MLPANN-GA models was greater than RBFANN-GA models due to their higher R^2 and lower RMSE values. The MLPANN-GA resulted in more precise models than RBFANN-GA according to our experimental data for MLVSS concentration in the aeration tank. The results of MLPANN-GA did not fluctuate significantly for all models with single input variables and joint variables. The results of RBFANN-GA models were not the same as results of MLPANN-GA models because they fluctuated for few variables due to the number of samples provided to the RBFANN-GA. We concluded that with the increase in the number of input data sets to train the ANNs, both RBFANN-GA and MLPANN-GA will show more reliable and similar models. In addition, it was observed that the precision of RBFANN-GA and MLPANN-GA models is determined not only by the number of input data to train the ANNs but also by the correlation of these data sets. The high correlation of the input data affected the MLPANN-GA models more than RBFANN-GA models, while the number of the input data affected the RBFANN-GA models more than MLPANN-GA models. At the same time, the perfection and precision of data influence the applicability of the models. As a result, the applicability of the models allows a feasible way for on-line control of the process [41].

The results indicated that the MLPANN-GA has stronger approximation and generalization ability than the RBFANN-GA with regard to our experimental data sets for MLVSS concentration in the aeration tank. The results of the MLVSS modeling using the RBFANN-GA and MLPANNGA for all data were highly collaborated with previous studies [2,31]. The simulation of MLVSS concentration in the aeration tank was successful for both RBFANN-GA and MLPANN-GA models. Both models showed an almost perfect match between the experimental and the simulated values of MLVSS. Based on the results of ANN modeling for all data sets, it was observed that the precision of RBFANN-GA and MLPANN-GA models is determined not only by the number of input variables of the network but also by the correlation of these variables. The high correlation of the input data affected the MLPANN-GA models more than RBFANN-GA models. On the other hand, the number of the input data affected the RBFANN-GA models more than MLPANN-GA models. Fig. 4 shows the regression lines for all data sets based on RBFANN-GA and MLPANN-GA models for MLVSS concentration in the aeration tank. The values of R^2 for MLVSS

Table 4
Effect of different single and joint variables on MLVSS in the aeration tank

	RBFANN-GA models for MLVSS				MLPANN-GA models for MLVSS				
	R^2		RMSE (mg/L)		R^2		RMSE (mg/L)		
Input variable no.	Train	Test	Train	Test	Train	Test	Train	Test	Importance order
1	0.44	0.33	558	615	0.47	0.32	546	611	5
2	0.64	0.51	435	447	0.64	0.63	430	435	3
3	0.77	0.74	397	406	0.78	0.74	390	401	2
4	0.55	0.43	476	534	0.58	0.51	461	497	4
5	0.78	0.76	384	391	0.78	0.77	381	387	1
5–1	0.66	0.54	351	414	0.67	0.61	307	376	4
5–2	0.82	0.81	237	242	0.89	0.86	207	221	2
5–3	0.89	0.85	192	201	0.91	0.89	178	192	1
5–4	0.77	0.64	279	339	0.87	0.75	245	312	3
5–3–1	0.88	0.81	154	162	0.88	0.85	140	148	3
5–3–2	0.94	0.91	101	132	0.95	0.93	95	126	2
5–3–4	0.94	0.91	96	125	0.96	0.93	94	120	1
5–3–4–1	0.94	0.91	100	127	0.94	0.91	93	121	2
5–3–4–2	0.95	0.92	95	123	0.95	0.92	90	116	1
5–3–4–2–1	0.96	0.93	92	120	0.98	0.95	85	104	1

Note: The numbers 1 to 5 refers to input variables identified in Table 3.

models by RBFANN-GA and MLPANN-GA were 0.94404 and 0.96355, respectively, compared to the findings of Moral et al., in which R^2 varied from 0.81 to 0.98 [2]. The residuals of models attained by RBFANN-GA and MLPANN-GA for all data were plotted out vs. the frequency of data in Fig. 4. A normal distribution of variation results in a Gaussian curve (specific bell-shaped curve), with the highest point in the middle and smoothly curving symmetrical slopes on both sides of center. This figure illustrates an approximately normal distribution of residuals produced by RBFANN-GA and MLPANN-GA models. Gaussian curve reveals our results are symmetrical and their axis round around zero for all data sets [42].

In GA-based ANNs, GA is used to optimize the weights and thresholds of back-propagation ANN for minimizing the error between the actual and target outputs [37]. RBFANN and MLPANN were optimized with GA because GA is good at efficiently searching large and complex spaces to find nearly global optima. GA indicates an increasingly attractive alternative to gradient-based techniques such as RBFANN and MLPANN as the complexity of the search space increases. The results showed that the precision and accuracy of all ANN models increased when GA is applied to the ANN models. The values of R^2 for all, train, and test models by RBFANN-GA were 0.97, 0.96, and 0.93, respectively comparing with the values of R^2 for all, train and test models by RBFANN which were 0.89, 0.84, and 0.81, respectively. The values of RMSE for all, train, and test models by RBFANN-GA were 88, 92, and 120 mg/L, respectively, compared with the values of RMSE for all, train, and test models by RBFANN which were 106, 117, and 155 mg/L, respectively. The values of R^2 for all, train, and test models by MLPANN-GA were 0.99, 0.98, and 0.95, respectively, compared with the values of R^2 for all, train, and test models by MLPANN which were 0.90, 0.86, and 0.85, respectively. The values of RMSE for all, train, and test models by MLPANN-GA were 84, 85, and 105 mg/L, respectively, compared with the values of RMSE for all, train, and test models by MLPANN which were 99, 108, and 147 mg/L, respectively.

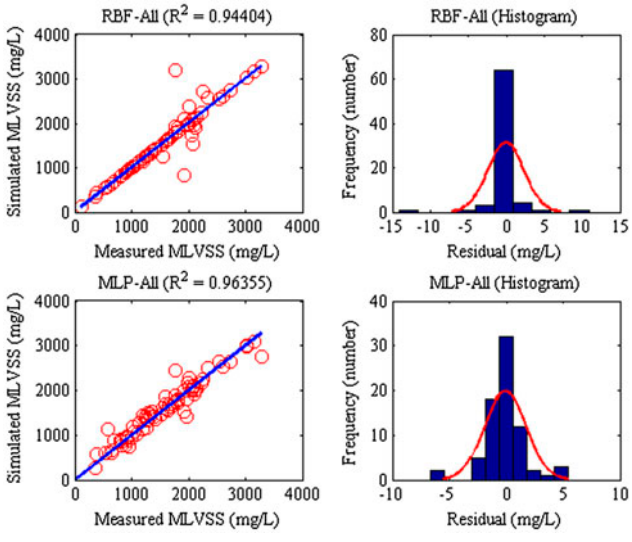

Fig. 4. Regression plots and residuals of RBFANN-GA and MLPANN-GA for MLVSS prediction based on all data sets.

3.3. Prediction and analysis of effluent COD, TN, and TSS

In order to predict the effluent COD, TN, and TSS concentrations by RBFANN-GA and MLPANN-GA, the pH, T (°C), influent concentrations of COD, TN or TSS, SVI, and V30 were considered as inputs of the networks. The results of the effluent COD, TN, and TSS modeling using the RBFANN-GA and MLPANNGA for training and testing data were highly collaborated with previous studies [9,14,16]. The training procedures for prediction of the effluent COD, TN, and TSS concentrations were successful for both RBFANN-GA and MLPANN-GA models. The train and test models by RBFANN-GA and MLPANN-GA indicated an almost perfect match between the experimental and the predicted values of the effluent COD, TN, and TSS. The results of ANN modeling showed that the MLPANN-GA has stronger approximation and generalization ability than the RBFANN-GA according to our experimental training and testing data sets for effluent COD, TN, and TSS. The results of ANN modeling for the effluent COD, TN, and TSS indicated that the precision of RBFANN-GA and MLPANN-GA models is determined not only by the number of input variables of the network but also by the correlation of these variables. The high correlation of the input data affected the MLPANN-GA models more than RBFANN-GA models. On the other hand, the number of the input data affected the RBFANN-GA models more than MLPANN-GA models.

The R^2 values of train models by RBFANN-GA for effluent COD, TN, and TSS were 0.98137, 0.99014, and 0.98021, respectively, and for the test (verification) models were 0.97232, 0.98325, and 0.95217. The R^2 values of train models by MLPANN-GA for effluent COD, TN, and TSS were 0.99017, 0.99047, and 0.98486, respectively, and for the test (verification) models were 0.98044, 0.98479, and 0.95484. The results show a good fitting between predicted values of effluent

Table 5
Effect of different single and joint variables on the effluent of COD, TN, and TSS

	RBFANN-GA models				MLPANN-GA models				
	R^2		RMSE (mg/L)		R^2		RMSE (mg/L)		
Input variable no.	Train	Test	Train	Test	Train	Test	Train	Test	Importance order
Models of effluent COD concentration									
1	0.33	0.44	21.34	22.14	0.39	0.71	19.72	13.92	5
2	0.47	0.46	18.65	20.52	0.59	0.86	17.34	11.28	3
3	0.77	0.86	14.81	12.28	0.88	0.91	12.73	10.23	1
4	0.43	0.44	20.64	21.97	0.49	0.78	18.75	12.97	4
5	0.69	0.61	15.38	16.15	0.67	0.91	15.14	10.44	2
Models of effluent TN concentration									
1	0.21	0.19	1.12	1.25	0.21	0.21	1.05	1.14	5
2	0.42	0.47	0.91	0.81	0.45	0.49	0.87	0.71	3
3	0.87	0.86	0.49	0.49	0.87	0.88	0.49	0.42	1
4	0.32	0.35	0.99	0.93	0.33	0.38	0.96	0.87	4
5	0.61	0.55	0.78	0.76	0.69	0.88	0.67	0.62	2
Models of effluent TSS concentration									
1	0.29	0.21	15.65	16.97	0.37	0.25	14.07	15.52	5
2	0.37	0.35	14.17	12.02	0.41	0.39	13.23	11.47	4
3	0.76	0.77	5.51	6.17	0.79	0.81	5.14	5.58	1
4	0.49	0.52	12.14	11.28	0.54	0.61	11.24	10.58	3
5	0.57	0.59	11.12	10.18	0.71	0.73	10.04	9.82	2

Note: The numbers 1 to 5 refers to input variables identified in Table 3.

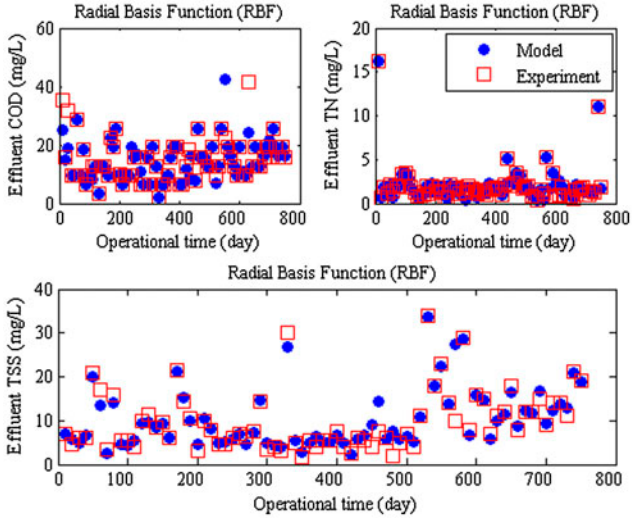

Fig. 5. Effluent COD, TN, and TSS models by RBFANN-GA based on all data sets.

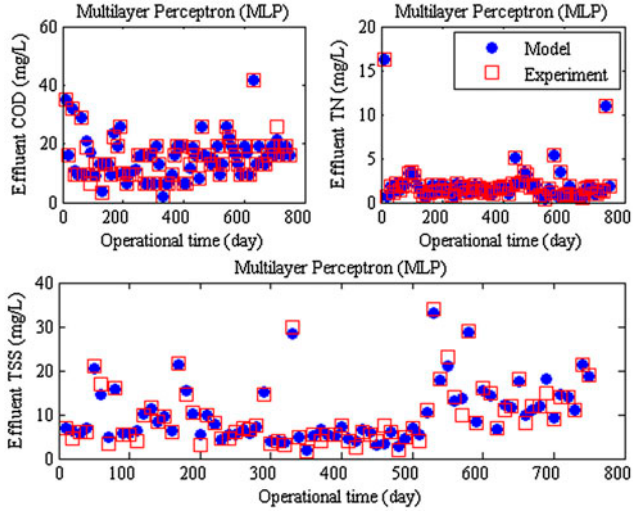

Fig. 6. Effluent COD, TN, and TSS models by MLPANN-GA based on all data sets.

COD, TN, and TSS by RBFANN-GA and MLPANN-GA and experimental values for various inputs. The coefficient of determination in this study for the effluent COD, TN, and TSS models improved results of previous studies [9,14,16], which indicated that in the sample data simulation, the ANN had good generation ability, with R^2 varying from 0.5 to 0.93. A set of COD, TN, and TSS data was used to examine

the predictive ability of the ANN models in order to verify our models. The RMSE values of train models by RBFANN-GA for effluent COD, TN, and TSS were 1.95, 0.164, and 2.56 mg/L, respectively, and for the test (verification) models were 1.78, 0.133, and 2.27 mg/L. The RMSE values of train models by MLPANN-GA for effluent COD, TN, and TSS were 1.54, 0.144, and 2.42 mg/L, respectively, and for the test (verification) models were 1.42, 0.112, and 2.13 mg/L. The mean squared error (MSE) values obtained for training and test sets with the ANNs selected to predict the effluent COD, TN, and TSS varied from 0.224 to 15 in the previous researches [14,16]. The mean average error in prediction of effluent COD, TN, and TSS by RBFANN-GA and MLPANN-GA for train and test models did not exceed 6 and 4%, respectively.

The effluent COD, TN, and TSS were modeled separately by considering various single variables as inputs of RBFANN-GA and MLPANN-GA in order to examine the effects of each variable on the changes of effluent COD, TN, and TSS concentrations. When the number of process variables is high, the extraction of relationships among process variables is not an easy task [43]. We have indicated that analysis of variables using ANN separate models offers a convenient way to examine the effects of the process variables at once and acts as a very effective tool to find the relationships among high-dimensional process variables in the activated sludge WWTPs. Table 5 shows the importance order of each input variable for the prediction of effluent COD, TN, and TSS concentrations. The results of RBFANN-GA and MLPANN-GA models showed that the variation of the effluent COD concentration is influenced by influent COD, V30, T (°C), SVI, and pH. This research indicates that the influent COD and V30 significantly affect the effluent COD concentration. In addition, the results indicated that the variation of the effluent TN concentration is influenced by influent TN, V30, T (°C), pH, and SVI. This research indicates that the influent TN and V30 significantly affect the effluent TN concentration. The results of RBFANN-GA and MLPANN-GA models indicated that the variation of the effluent TSS concentration is influenced by influent TSS, SVI, V30, T (°C), and pH. This research indicates that the influent TSS and SVI significantly affect the effluent TSS concentration.

The results of the effluent COD, TN, and TSS modeling using the RBFANN-GA and MLPANNGA for all data were highly collaborated with previous studies [2,31]. Figs. 5 and 6 show that the prediction of effluent COD, TN, and TSS concentrations was successful for both RBFANN-GA and MLPANN-GA models. Both models showed an almost perfect match between the experimental and the predicted values of effluent COD, TN, and TSS. The results of this study indicated that the MLPANN-GA has stronger approximation and generalization ability than the RBFANN-GA with regard to our experimental data sets for effluent COD, TN, and TSS.

4. Conclusions

A real-time monitoring system for WWTPs has been developed to give operators a guideline that would allow them to arrive at the optimal operational strategies in the early stage of a process disturbance. The most important aspect of ANNs is the ability of self-organization of the models, which show the advantages of intelligent modeling; it is rapid, easy to operate, non-invasive, and not expensive. In the current research, Ekbatan WWTP was modeled using RBFANN-GA and MLPANN-GA. Temperature, pH, influent concentration of contaminants, SVI, and V30 were inputs of the neural networks. These input variables were used to predict effluent COD, TN, and TSS concentrations as well as MLVSS concentration in the aeration tank. The RBFANN-GA applied network function of newrbe to the input data with the spread of radial basis function equal to 1. The MLPANN-GA applied network function of newff to the input data. The MLPANN-GA was trained by different learning algorithms for maximum 400 epochs. Nevertheless, the LM algorithm resulted in the optimal models for training and testing data after less than 20 iterations. Based on our research, the optimal models were obtained with the hidden layer consisting of 10 neurons. The best transfer function for the hidden layer was found to be hyperbolic tangent sigmoid (tansig) function while the best transfer function for the output layer was a linear one (purelin).

The training procedures of all contaminants were highly collaborated for both RBFANN-GA and MLPANN-GA models. The results of training and testing data sets indicated an almost perfect match between the experimental and the predicted values of COD, TN, TSS, and MLVSS for both RBFANN-GA and MLPANN-GA models. The results showed that with low values of input data to train ANNs, the MLPANN-GA models compared to RBFANN-GA models are more precise due to their higher R^2 and lower RMSE values. The values of R^2 for train and test (verification) models by RBFANN-GA and MLPANN-GA varied from 0.93 to 0.99. The mean average error in simulation of all contaminants for train and test models did not exceed 6 and 4%, respectively. It was observed that accuracy of all ANN models increased when GA was applied to the ANN models.

Acknowledgments

The authors are grateful to Ekbatan wastewater treatment plant for their technical and logistical assistance during this work which was supported by authors. The authors declare that they have no competing interests.

Nomenclature

ASM	—	activated sludge model
ASP	—	activated sludge process
WWTP	—	wastewater treatment plant
ANN	—	artificial neural network
MLP	—	multi-layer perceptron
RBF	—	radial basis function
RNN	—	recurrent neural network
ESN	—	echo-state networks
MLPANN	—	multi-layer perceptron artificial neural network
BOD	—	biochemical oxygen demand
COD	—	chemical oxygen demand
TSS	—	total suspended solids
RBFANN	—	radial basis function artificial neural network
DO	—	dissolved oxygen
GA	—	genetic algorithm
MLVSS	—	mixed liquor volatile suspended solids
TN	—	total nitrogen
T	—	temperature
SVI	—	sludge volume index
V30	—	sludge volume after 30 min of settling
A2O	—	anaerobic-anoxic-oxic
HRT	—	hydraulic retention time
TDS	—	total dissolved solids
MLSS	—	mixed liquor suspended solids
R^2	—	coefficient of determination
RMSE	—	root-mean-squared error
GDB	—	gradient descent back-propagation
LM	—	Levenberg–Marquardt
FBNN	—	feed-forward back-propagation neural network
MSE	—	mean squared error

References

[1] Y. Du, R. Tyagi, R. Bhamidimarri, Use of fuzzy neural-net model for rule generation of activated sludge process, Process Biochem. 35 (1999) 77–83.
[2] H. Moral, A. Aksoy, C.F. Gokcay, Modeling of the activated sludge process by using artificial neural networks with automated architecture screening, Comput. Chem. Eng. 32 (2008) 2471–2478.
[3] K.V. Gernaey, M. van Loosdrecht, M. Henze, M. Lind, S.B. Jørgensen, Activated sludge wastewater treatment plant modelling and simulation: State of the art, Environ. Model. Softw. 19 (2004) 763–783.
[4] M. Bagheri, S.A. Mirbagheri, A.M. Kamarkhani, Z. Bagheri, Modeling of effluent quality parameters in a submerged membrane bioreactor with simultaneous upward and downward aeration treating municipal wastewater using hybrid models, Desalin. Water Treat. (2015) 1–22, doi: 10.1080/19443994.2015.1021852.
[5] M. Henze, W. Gujer, T. Mino, T. Matsuo, M. Wentzel, G. Marais, Wastewater and biomass characterization for the activated sludge model no. 2: Biological phosphorus removal, Water Sci. Technol. 31 (1995) 13–23.
[6] L. Chen, Y. Tian, C. Cao, S. Zhang, S. Zhang, Sensitivity and uncertainty analyses of an extended ASM3-SMP model describing membrane bioreactor operation, J. Membr. Sci. 389 (2012) 99–109.
[7] M.W. Lee, S.H. Hong, H. Choi, J.-H. Kim, D.S. Lee, J.M. Park, Real-time remote monitoring of small-scaled biological wastewater treatment plants by a multivariate statistical process control and neural network-based software sensors, Process Biochem. 43 (2008) 1107–1113.
[8] B. Ráduly, K.V. Gernaey, A. Capodaglio, P.S. Mikkelsen, M. Henze, Artificial neural networks for rapid WWTP performance evaluation: Methodology and case study, Environ. Model. Softw. 22 (2007) 1208–1216.
[9] T. Pai, Y. Tsai, H. Lo, C. Tsai, C. Lin, Grey and neural network prediction of suspended solids and chemical oxygen demand in hospital wastewater treatment plant effluent, Comput. Chem. Eng. 31 (2007) 1272–1281.
[10] H.-G. Han, J.-F. Qiao, Prediction of activated sludge bulking based on a self-organizing RBF neural network, J. Process Control 22 (2012) 1103–1112.
[11] H.-W. Chen, R.-F. Yu, S.-K. Ning, H.-C. Huang, Forecasting effluent quality of an industry wastewater treatment plant by evolutionary grey dynamic model, Resour. Conserv. Recycl. 54 (2010) 235–241.
[12] A. Zilouchian, M. Jafar, Automation and process control of reverse osmosis plants using soft computing methodologies, Desalination 135 (2001) 51–59.
[13] G. Zeng, X. Qin, L. He, G. Huang, H. Liu, Y. Lin, A neural network predictive control system for paper mill wastewater treatment, Eng. Appl. Artif. Intell. 16 (2003) 121–129.
[14] M.S. Nasr, M.A. Moustafa, H.A. Seif, G. El Kobrosy, Application of Artificial Neural Network (ANN) for the prediction of EL-AGAMY wastewater treatment plant performance-EGYPT, Alexandria Eng. J. 51 (2012) 37–43.
[15] B. Suchacz, M. Wesołowski, The recognition of similarities in trace elements content in medicinal plants using MLP and RBF neural networks, Talanta 69 (2006) 37–42.
[16] F.S. Mjalli, S. Al-Asheh, H. Alfadala, Use of artificial neural network black-box modeling for the prediction of wastewater treatment plants performance, J. Environ. Manage. 83 (2007) 329–338.
[17] H.-G. Han, J.-F. Qiao, Q.-L. Chen, Model predictive control of dissolved oxygen concentration based on a self-organizing RBF neural network, Control Eng. Pract. 20 (2012) 465–476.
[18] M.F. Hamoda, I.A. Alghusain, A.H. Hassan, Integrated wastewater treatment plant performance evaluation using artificial neural networks, Water Sci. Technol. 40 (1999) 55–65.

[19] L. Luccarini, G.L. Bragadin, G. Colombini, M. Mancini, P. Mello, M. Montali, D. Sottara, Formal verification of wastewater treatment processes using events detected from continuous signals by means of artificial neural networks. Case study: SBR plant, Environ. Model. Softw. 25 (2010) 648–660.
[20] D. Hanbay, I. Turkoglu, Y. Demir, Prediction of wastewater treatment plant performance based on wavelet packet decomposition and neural networks, Expert Syst. Appl. 34 (2008) 1038–1043.
[21] C. Gontarski, P. Rodrigues, M. Mori, L. Prenem, Simulation of an industrial wastewater treatment plant using artificial neural networks, Comput. Chem. Eng. 24 (2000) 1719–1723.
[22] R. Badrnezhad, B. Mirza, Modeling and optimization of cross-flow ultrafiltration using hybrid neural network-genetic algorithm approach, J. Ind. Eng. Chem. 20(2) (2014) 528–543, doi: 10.1016/j.jiec.2013.05.012.
[23] M. Sarma, V. Sahai, V. Bisaria, Genetic algorithm-based medium optimization for enhanced production of fluorescent pseudomonad R81 and siderophore, Biochem. Eng. J. 47 (2009) 100–108.
[24] W. Kurek, A. Ostfeld, Multi-objective optimization of water quality, pumps operation, and storage sizing of water distribution systems, J. Environ. Manage. 115 (2013) 189–197.
[25] S.M.S. Abkenar, S.D. Stanley, C.J. Miller, D.V. Chase, S.P. McElmurry, Evaluation of genetic algorithms using discrete and continuous methods for pump optimization of water distribution systems, Sustain. Comput.: Inform. Syst. 8 (2014) 18–23, doi: 10.1016/j.suscom.2014.09.003.
[26] H. Mehmood, N.K. Tripathi, Cascading artificial neural networks optimized by genetic algorithms and integrated with global navigation satellite system to offer accurate ubiquitous positioning in urban environment, Comput. Environ. Urban Syst. 37 (2013) 35–44.
[27] D. Andrew, Standard Methods for the Examination of Water and Wastewater, APHA-AWWA-WEF, Washington, DC, 2005.
[28] I. Metcalf, Wastewater Engineering; Treatment and Reuse, McGraw-Hill, Boston, MA, 2003.
[29] M. Khayet, C. Cojocaru, Artificial neural network modeling and optimization of desalination by air gap membrane distillation, Sep. Purif. Technol. 86 (2012) 171–182.
[30] M. Kashaninejad, A. Dehghani, M. Kashiri, Modeling of wheat soaking using two artificial neural networks (MLP and RBF), J. Food Eng. 91 (2009) 602–607.
[31] A.R. Pendashteh, A. Fakhru'l-Razi, N. Chaibakhsh, L.C. Abdullah, S.S. Madaeni, Z.Z. Abidin, Modeling of membrane bioreactor treating hypersaline oily wastewater by artificial neural network, J. Hazard. Mater. 192 (2011) 568–575.
[32] S.S. Madaeni, N.T. Hasankiadeh, A.R. Kurdian, A. Rahimpour, Modeling and optimization of membrane fabrication using artificial neural network and genetic algorithm, Sep. Purif. Technol. 76 (2010) 33–43.
[33] D. Prakotpol, T. Srinophakun, GAPinch: Genetic algorithm toolbox for water pinch technology, Chem. Eng. Process. 43 (2004) 203–217.
[34] U. Kılıç, K. Ayan, U. Arifoğlu, Optimizing reactive power flow of HVDC systems using genetic algorithm, Int. J. Electr. Power Energy Syst. 55 (2014) 1–12.
[35] I. Rocha, E. Parente Jr., A. Melo, A hybrid shared/distributed memory parallel genetic algorithm for optimization of laminate composites, Compos. Struct. 107 (2014) 288–297.
[36] N. Gupta, G.S. Gaba, H.S. Gill, A new approach for function optimization using hybrid GA-ANN algorithm, Int. J. Eng. Res. Appl. 2 (2012) 386–389.
[37] Z. Yuan, L.-N. Wang, X. Ji, Prediction of concrete compressive strength: Research on hybrid models genetic based algorithms and ANFIS, Adv. Eng. Softw. 67 (2014) 156–163.
[38] J.D. Dyer, R.J. Hartfield, G.V. Dozier, J.E. Burkhalter, Aerospace design optimization using a steady state real-coded genetic algorithm, Appl. Math. Comput. 218 (2012) 4710–4730.
[39] G.B. Sahoo, C. Ray, Predicting flux decline in cross-flow membranes using artificial neural networks and genetic algorithms, J. Membr. Sci. 283 (2006) 147–157.
[40] A. Saltelli, M. Ratto, T. Andres, F. Campolongo, J. Cariboni, D. Gatelli, M. Saisana, S. Tarantola, Introduction to sensitivity analysis, in: Global Sensitivity Analysis: The Primer, John Wiley & Sons, Chichester, 2007.
[41] S. Grieu, A. Traoré, M. Polit, J. Colprim, Prediction of parameters characterizing the state of a pollution removal biologic process, Eng. Appl. Artif. Intell. 18 (2005) 559–573.
[42] A. Chamkalani, M. Amani, M.A. Kiani, R. Chamkalani, Assessment of asphaltene deposition due to titration technique, Fluid Phase Equilib. 339 (2013) 72–80.
[43] Y.-S.T. Hong, M.R. Rosen, R. Bhamidimarri, Analysis of a municipal wastewater treatment plant using a neural network-based pattern analysis, Water Res. 37 (2003) 1608–1618.